Chapter 3

Theory of Phase Noise Mechanism of NEMS

We present the theory of phase noise mechanism of NEMS. We examine both fundamental and nonfundamental noise processes to obtain expressons for phase noise density, Allan deviation, and mass sensitivity. Fundamental noise processes considered here include thermomechanical noise, momentum exchange noise, adsorption-desorption noise, diffusion noise, and temperature fluctuation noise. For nonfundamental noise processes, we develop a formalism to consider the Nyquist-Johnson noise from transducer amplifier implementations. The detailed analysis here not only reveals the achievable frequency stability of NEMS devices, but also provides a theoretical framework to fully optimize noise performance and the mass sensitivity for sensing applications.

3.1 Introduction

So far we have considered how physical fluctuations convert into the noise sidebands of the carrier and give the conventional definition of phase noise, frequency noise, and Allan deviation, all commonly used to characterize the frequency stability of an oscillator. Here we proceed to investigate phase noise mechanisms affecting NEMS devices. First, we examine the *fundamental* noise processes intrinsic to NEMS devices.[1-3] We begin our discussion from thermomechanical noise, originating from thermally driven random motion of the resonator, by considering the thermal fluctuating force acting on the resonator. We then consider momentum exchange noise, adsorption-desorption noise, and diffusion noise, all arising from gaseous molecules in resonator surroundings. The impinging gaseous molecules can impart momentum randomly to a NEMS device and induce momentum exchange noise. Moreover, when gaseous species adsorb on a NEMS device, typically from the surrounding environment, they can diffuse along the surface in and out of the device and produce diffusion noise. Meanwhile, they can also briefly reside on the surface and then desorb again and generate adsorption-desorption noise. We also discuss the noise due to the temperature fluctuations; these fluctuations are fundamental to any object with finite thermal conductance and are distinct from environmental drifts that can be controlled using oven-heated packaging, similar to that used for high precision quartz clocks.

Note that the thermomechanical noise from the internal loss mechanism in the resonator and the momentum exchange noise from gaseous damping are dissipation-induced fluctuations. They are expected for mechanical resonators with nonzero dissipation according to the fluctuation-dissipation theorem.[4] Other noise sources

including adsorption-desorption noise, diffusion noise, and temperature fluctuation noise are parametric noise. These have to do with parametric changes in the physical properties of the resonator such as device mass and temperature, which cause the natural resonance frequency of the resonator to change, but do not necessarily involve energy dissipation, leaving the quality factor unchanged.[1]

Finally, we consider the nonfundamental noise processes from the readout circuitry of transducer implementations.[5] In general, the NEMS transducers covert mechanical displacement into an electrical signal, which is subsequently amplified to the desired level by an amplifier for readout. Hence both the transducer and amplifier can add extrinsic noise to the NEMS devices, and the impact on frequency fluctuations is treated by our formalism developed here. Our formalism will reveal the resulting impact on the frequency fluctuations and enable the optimization of noise performance. Although we focus our discussion on the Nyquist-Johnson noise from the transducer and readout amplifier implementations, it can be readily generalized to incorporate other types of extrinsic noise such as flicker noise.

In conjunction with the discussion of each noise process, we also give the expression for the corresponding mass sensitivity limit. In general, resonant mass sensing is performed by carefully determining the resonance frequency ω_0 of the resonator and then, by looking for a frequency shift in the steady state due to the accreted mass. Therefore, the minimum measurable frequency shift, $\delta\omega_0$, will translate into the minimum measurable mass, δM, referred to as the mass sensitivity, δM. Henceforth, we model the resonator as a one-dimensional simple harmonic oscillator characterized by the

effective mass M_{eff} and the dynamic stiffness $\kappa_{eff} = M_{eff} \omega_0^2$.[6] Assuming that δM is a small fraction of M_{eff}, we can write a linearized expression

$$\delta M \approx \frac{\partial M_{eff}}{\partial \omega_0} \delta \omega_0 = \Re^{-1} \delta \omega_0 . \tag{3.1}$$

This expression assumes that the modal quality factor and compliance are not appreciably affected by the accreted species. This is consistent with the aforementioned presumption that $\delta M \ll M_{eff}$. Apparently, δM critically depends on the minimum measurable frequency shift $\delta \omega_0$ and the inverse mass responsivity $\Re^{-1}$. Since κ_{eff} for the employed resonant mode—a function of the resonator's elastic properties and geometry—is unaffected by small mass changes, we can further determine that

$$\Re = \frac{\partial \omega_0}{\partial M_{eff}} = -\frac{\omega_0}{2M_{eff}} , \tag{3.2}$$

$$\delta M \approx -2 \frac{M_{eff}}{\omega_0} \delta \omega_0 . \tag{3.3}$$

We note that equation (3.3) is analogous to the Sauerbrey equation,[7] but is instead here written in terms of the absolute mass, rather than the mass density, of the accreted species. Both fundamental and nonfundamental noise processes will impose limits on $\delta \omega_0$, and therefore on δM. For each noise process, we will integrate phase noise density to obtain the expression for $\delta \omega_0$ by using equation (2.25) and translate it into δM using equation (3.3).[3]

3.2 Thermomechanical Noise

We now consider the thermomechanical noise, originating from thermally driven random motion of NEMS devices.[1-3] For the one-dimensional simple harmonic oscillator, the mean square displacement fluctuations of the center of mass, $\langle x_{th} \rangle$, satisfy $M_{eff}\omega_0^2 \langle x_{th}^2 \rangle / 2 = k_B T / 2$. Here, k_B is Boltzmann's constant and T is the resonator temperature. The spectral density of these random displacements, $S_x(\omega)$, (with units of m^2/Hz) is given by

$$S_x(\omega) = \frac{1}{M_{eff}^2} \frac{S_F(\omega)}{(\omega^2 - \omega_0^2)^2 + \omega^2 \omega_0^2 / Q^2}. \tag{3.4}$$

The thermomechanical force spectral density in units of N^2/Hz has a white spectrum $S_F(\omega) = 4M_{eff}\omega_0 k_B T / Q$. For $\omega \gg \omega_0 / Q$, the phase noise density is given by the expression[1]

$$S_\phi(\omega) = \frac{1}{2} \frac{S_x(\omega)}{|x_C|^2} = \frac{k_B T}{8\pi P_C} \left(\frac{\omega_0}{\omega} \right)^2. \tag{3.5}$$

P_C is the maximum carrier power, limited by onset of non-linearity of mechanical vibration of the NEMS. For a doubly clamped beam with rectangular cross section driven into flexural resonance, the non-linearity results from Duffing instability and the maximum carrier power can be estimated by $P_C = \omega_0 E_C / Q = M_{eff}\omega_0^3 |x_C|^2 / Q$ with critical amplitude $|x_C|$ given by $t / \sqrt{Q(1 - v^2)}$ for doubly clamped beams.[8] t is the dimension of the beam in the direction of transverse vibration; v is the Poisson ratio of the beam material.[9]

Upon direct integration of the spectral density, Allan deviation is given by

$$\sigma_A(\tau_A) = \sqrt{\frac{k_B T}{8 P_C Q^2 \tau_A}}.$$ (3.6)

We can rewrite this expression in terms of the ratio of the maximum drive (carrier) energy, $E_C = M_{eff}\omega_0^2 |x_C|^2$, to the thermal energy, $E_{th} = k_B T$, representing the effective dynamic range intrinsic to the device itself. This is the signal-to-noise ratio (SNR) available for resolving the coherent oscillatory response above the thermal displacement fluctuations. We can express this dynamic range, as is customary, by $DR(dB) = 10\log(E_C / k_B T)$ in units of decibels. This yields a very simple expression

$$\sigma_A(\tau_A) = (1/\tau_A Q \omega_0)^{1/2} 10^{-DR/20}.$$ (3.7)

We now turn to the evaluation of the minimum measurable frequency shift, $\delta\omega_0$, limited by thermomechanical fluctuations of a NEMS resonator. To obtain $\delta\omega_0$, the integral in equation (2.25) must be evaluated using the expression for $S_\omega(\omega)$ given in equation (3.5) over the effective measurement bandwidth. Performing this integration for the case where $Q>>1$ and $2\pi\Delta f << \omega_0 / Q$, we obtain:

$$\delta\omega_0 \approx \left[\frac{k_B T}{E_C}\frac{\omega_0 \Delta f}{Q}\right]^{1/2},$$ (3.8)

$$\delta M \approx 2 M_{eff}\left(\frac{E_{th}}{E_c}\right)^{1/2}\left(\frac{\Delta f}{Q \omega_0}\right)^{1/2}.$$ (3.9)

We can also recast equation (3.9) in terms of dynamic range *DR* and mass responsivity $\Re$ as

$$\delta M \approx \frac{1}{\Re}\left(\Delta f \frac{\omega_0}{Q}\right)^{1/2} 10^{(-DR/20)}.$$ (3.10)

Note that Q/ω_0 is the open-loop response (ring-down) time of the resonator. In table 3.1, we have translated these analytical results from equation (3.7) and equation (3.9) into

34

concrete numerical estimates for representative realizable device configurations. We list the Allan deviation σ_A (for averaging time τ_A=1 sec) and the mass sensitivity δM (for measurement bandwidth Δf =1 kHz), limited by thermomechancial noise, for three representative device configurations with quality factor Q=10^4. For the calculation of resonant frequency, we assume Young's modulus E=169 GPa and mass density ρ=2.33 g/cm^3 for the silicon beam and silicon nanowire and E= 1 TPa and ρ= 1g/cm^3 for the single walled nanotube (SWNT). First, a large dynamic range is always desirable for obtaining frequency stability in the case of thermomechanical noise. Clearly, as the device sizes are scaled downward while maintaining high resonance frequencies, M_{eff} and κ_{eff} must shrink in direct proportion. Devices with small stiffness (high compliance) are more susceptible to thermal fluctuations and consequently, the dynamic range becomes reduced. Second, the values of the mass sensitivity span only the regime from a few tenths to a few tens of Daltons. This is the mass range for a small *individual* molecule or atom; hence it is clear that nanomechanical mass sensors offer unprecedented ability to *weigh* individual neutral molecules or atoms and will find many interesting applications in mass spectrometry and atomic physics.[10,11]

Device	Frequency	Dimensions ($L \times w \times t$)	M_{eff}	DR	σ_A (1sec)	δM (1kHz)
Si beam	1 GHz	660 nm $\times$ 50 nm $\times$ 50 nm	2.8 fg	66 dB	3.2×10^{-10}	7.0 Da
Si nanowire	7.7 GHz	100 nm $\times$ 10 nm $\times$ 10 nm	17 ag	47 dB	9.5×10^{-10}	0.13 Da
SWNT	10 GHz	56 nm $\times$ 1.2 nm(dia.)	165 ag	14 dB	7.4×10^{-8}	0.05 Da

Table 3.1. Allan deviation and mass sensitivity limited by thermomechanical noise for representative realizable NEMS device configurations

3.3 Momentum Exchange Noise

We now turn to a discussion of the consequences of momentum exchange in a gaseous environment between the NEMS resonator and the gas molecules that impinge upon it. Gerlach first investigated the effect of a rarefied gas surrounding a resonant torsional mirror.[12] Subsequently, Uhlenbeck and Goudmit calculated the spectral density of the fluctuating force acting upon the mirror due to these random collisions.[13] Following these analyses, Ekinci et al. have obtained the mass sensitivity of the NEMS limited by momentum exchange noise.[3] Here we reproduce a similar version of their discussions. In the molecular regime at low pressure, the resonator's equation of motion is given by

$$M_{eff}\,\ddot{x} + \left(M_{eff}\frac{\omega_0}{Q_i} + \frac{pA_D}{v} \right)\dot{x} + M_{eff}\,\omega_0^2 x = F(t).$$ (3.11)

The $(M_{eff}\omega_0/Q_i)\dot{x}$ term results from the intrinsic loss mechanism. The term $(pA_D/v)\dot{x}$ represents the drag force due to the gas molecules. P is the pressure, A_D is the device surface area, and $v = \sqrt{k_B T/m}$ is the thermal velocity of gas molecule. The quality factor due to gas dissipation can be defined as $Q_{gas} = MvPA_D$. The loaded quality factor Q_L, as a result of two dissipation mechanisms, can be defined as $Q_L^{-1} = Q_i^{-1} + Q_{gas}^{-1}$. Since we have treated the thermomechanical noise from the intrinsic loss mechanism, we assume that $Q_i \gg Q_{gas}$ and focus on the noise from gaseous damping. The collision of gas molecules produces a random fluctuating force with the spectral density given by[3]

$$S_F(\omega) = 4mvPA_D = \frac{4M\omega_0 k_B T}{Q_{gas}}.$$ (3.12)

Similar to equation (3.5) and equation (3.6), the resulting formulas for the phase noise density and the Allan deviation are

$$S_\phi(\omega) = \frac{k_B T}{8\pi P_C Q_{gas}^2} \left(\frac{\omega_0}{\omega}\right)^2,$$
(3.13)

$$\sigma_A = \sqrt{\frac{k_B T}{P_C} \frac{1}{Q_{gas}^2 \tau_A}}.$$

(3.14)

After taking similar steps leading to equation (3.9), we obtain

$$\delta M \approx 2 M_{eff} \left(\frac{E_{th}}{E_c}\right)^{1/2} \left(\frac{\Delta f}{Q_{gas}\omega_0}\right)^{1/2}.$$
(3.15)

3.4 Adsorption-Desorption Noise

Adsorption-desorption noise has been first discussed by Yong and Vig.[14] The resonator environment will always include a nonzero pressure of surface contaminated molecules. As the gas molecules adsorb and desorb on the resonator surface, they mass load the device randomly and cause the resonant frequency to fluctuate. Yong and Vig developed the model for noninteracting, completely localized monolayer adsorption, henceforth referred to as Yong and Vig's model. In addition to Yong and Vig's model, we present the ideal gas model for the case of noninteracting, completely delocalized adsorption. However, the extreme of completely localized or completely delocalized adsorption rarely occurs on real surfaces; the adsorption on real surfaces always lies between these two extremes.[15] Adsorbed gases molecules can interact with each other, resulting in phase transitions on the surface.[16] Instead of monolayer adsorption, multilayer

adsorption usually happens on real surfaces.[15] All these effects can further complicate the analysis of adsorption-desorption noise. The two models presented here, despite their simplicity, reveal valuable insight in the theoretical understanding of the adsorption-desorption noise.

In Yong and Vig's model, the assumption of localized adsorption means that the kinetic energy of the adsorbed molecule is much smaller than the depth of surface potential, and thus the adsorbed molecule is completely immobile in the later direction. Thus the concept of adsorption site on the surface is well defined. We further assume each site can accommodate only one molecule and consider the stochastic process of adsorption-desorption of each site. Consider a NEMS device surrounded by the gas with pressure, P, and temperature, T. From kinetic theory of gas, the adsorption rate of each site is given by the number of impinging atoms or molecules per unit time per unit area times the sticking coefficient, s, and the area per site A_{site}.

$$r_a = \frac{2}{5} \frac{P}{\sqrt{mkT}} sA_{site},$$ (3.16)

where P and T are the pressure and temperature of gas, respectively. In general, the sticking coefficient depends on temperature and gaseous species.[17] Here we assume that the sticking coefficient is independent of the temperature.

Once bound to the surface, a molecule desorbs at a rate

$$r_d = v_d \exp(-\frac{E_b}{kT}),$$ (3.17)

v_d is the desorption attempt frequency, typically of order 10^{13} Hz for a noble gas on a metallic surface, and E_b is the binding energy. For N molecules adsorbed on the surface, the total desorption rate for the whole device is Nr_d. Since each site can only

accommodate one molecule, the number of available sites for adsorption is N_a-N, so the total adsorption rate is $(N_a$-$N)r_a$. Equating these two rates, we obtain the number of adsorbed molecules

$$N = N_a \frac{r_a}{r_a + r_d} . \tag{3.18}$$

The average occupation probability f of a site is defined as the ratio of the adsorbed molecules to the total number of sites, N/N_a, and is given by $f = r_a /(r_a + r_d)$. Substitution of equation (3.16) and equation (3.17) into equation (3.18) yields the formula for the number of adsorbed molecules as a function of temperature, also known as the Langmuir adsorption isotherm.[16]

$$\frac{N}{N_a} = \frac{\frac{2}{5}\frac{p}{\sqrt{mkT}}\frac{s}{v_d}A_{site}\exp(\frac{E_b}{kT})}{\frac{2}{5}\frac{p}{\sqrt{mkT}}\frac{s}{v_d}A_{site}\exp(\frac{E_b}{kT})+1} = \frac{a(T)p}{1+a(T)p} , \tag{3.19}$$

$$a(T) = \frac{2}{5}\frac{P}{\sqrt{mkT}}\frac{s}{v_d}\exp(\frac{E_b}{kT}) . \tag{3.20}$$

We can rewrite equation (3.16) in terms of the gaseous flux, Φ_{flux}, given by

$$\Phi_{flux} = (2/5)(P/\sqrt{mkT}) .$$

$$\frac{N}{N_a} = \frac{\Phi_{flux}\frac{s}{v_d}A_{site}\exp(\frac{E_b}{kT})}{\Phi_{flux}\frac{s}{v_d}A_{site}\exp(\frac{E_b}{kT})+1} . \tag{3.21}$$

We derive the spectral density of the frequency noise by considering the stochastic process of the adsorption-desorption of each site, which can be described by a continuous time two state Markov chain.[14] Here we briefly sketch the derivation for a two state Markov chain.[18] Since each site can be occupied or unoccupied, we consider a

continuous time stochastic process $\{\zeta(t), t{>}0\}$, where the random variable $\zeta(t)$ can take either 0 (unoccupied) or 1 (occupied). The two rate constants of such a Markov chain are r_d, the rate from state 1 (occupied state) to state 0 (unoccupied), and r_a, the rate from state 0 (unoccupied state) to state 1 (occupied state). We define $P_{ij}(t)$ as the conditional probability that a Markov chain, presently in state i, will be in the state j after additional time t. Assuming that the site is initially occupied, we have initial condition, $P_{11}(0) = 1$, and for a two state system, $P_{10}(t) = 1 - P_{11}(t)$. The corresponding Kolmogorov's forward equation and its solution are given by[10]

$$\frac{dP_{11}}{dt} = r_d P_{10}(t) - r_a P_{11}(t), \tag{3.22}$$

$$P_{11}(t) = \frac{r_a}{r_a + r_d} + \frac{r_d}{r_a + r_d} e^{-(r_a+r_d)t} = f + (1-f)e^{-t/\tau_r}. \tag{3.23}$$

The correlation time τ_r is defined as $1/(r_a + r_d)$. The autocorrelation function can be found by calculating the expectation value of $\zeta(t+\tau)\zeta(t)$ from the conditional probability function. By definition, the autocorrelation function of $\zeta(t)$ is given by

$$R_{site}(\tau) = E[\zeta(t+\tau)\zeta(t)] = \sigma_{OCC}^2 e^{-|\tau|/\tau_r} + f. \tag{3.24}$$

$E[]$ denotes the expectation value of the random variable. Here for our purpose, we neglect the constant term f since this corresponds to the D.C. part of the spectra. σ_{OCC}^2 is the variance of occupational probability f, given by $\sigma_{OCC}^2 = f(1-f) = r_a r_d /(r_a + r_d)^2$. Note that σ_{OCC}^2 reaches a maximum for $f{=}0.5$ when the adsorption and desorption rates of the site are equal.

We apply the Wiener-Khintchine theorem to obtain the corresponding spectral density of $\zeta(t)$ for each site by performing the Fourier transform of equation (3.24).

$$S_\zeta(\omega) = \frac{2\sigma_{OCC}^2 \tau_r / \pi}{1 + (\omega \tau_r)^2}.$$ (3.25)

Each adsorbed molecule of mass m will contribute to fractional frequency change $m/2M_{eff}$. We obtain the spectral density of fractional frequency noise by simply summing the contribution from each individual site.

$$S_y(\omega) = \frac{2\sigma_{OCC}^2 N_a / \pi}{1 + (\omega \tau_r)^2} \left(\frac{m}{2M_{eff}} \right)^2.$$ (3.26)

Since the spectral density exhibits Lorentizian function form, we use equation (2.16) to obtain

$$\sigma_A(\tau_A) = \sqrt{N_a} \sigma_{OCC} \frac{m}{M_{eff}} \sqrt{F(\frac{\tau_r}{\tau_A})}.$$ (3.27)

$F(x)$ is the analytic function defined in equation (2.17). In the limit, $\tau_r \ll \tau_A$, equation (3.27) becomes

$$\sigma_A(\tau_A) = \sqrt{N_a} \sigma_{OCC} \frac{m}{M_{eff}} \sqrt{\frac{\tau_r}{2\tau_A}}.$$ (3.28)

In the other limit, $\tau_A \ll \tau_r$, equation (3.27) becomes

$$\sigma_A(\tau_A) = \sqrt{N_a} \sigma_{OCC} \frac{m}{M_{eff}} \sqrt{\frac{\tau_A}{6\tau_r}}.$$ (3.29)

In the ideal gas model, the assumption of delocalized adsorption means that the kinetic energy of the adsorbed molecule is much higher than the depth of the surface potential, and thus the adsorbed molecule is mobile in the lateral direction. The notion of adsorption site in Yong and Vig's model is not well defined.[14] We thus analyze the

kinetics of adsorption-desorption using the total adsorption and desorption rates of the adsorbed atoms on the device. The total adsorption rate of the device is given by the flux of molecules multiplied by the sticking coefficient s and the device area A_D,

$$R_a = \frac{2}{5}\frac{P}{\sqrt{mk_BT}}sA_D.$$ (3.30)

Once bound to the surface, the molecule desorbs at a rate given by $r_d = v_d \exp(-E_b/kT)$. The total desorption rate of all the adsorbed molecules on the device is simply

$$R_d = v_d \exp(-\frac{E_b}{kT})N.$$ (3.31)

At equilibrium, the total adsorption rate equals the total desorption rate, and the number of adsorbed molecules is given by

$$\frac{N}{A_D} = \frac{2}{5}\frac{s}{v_d}\frac{P}{\sqrt{mkT}}\exp(\frac{E_b}{kT}) = b(T)P,$$ (3.32)

$$b(T) = \frac{2}{5}\frac{s}{v_d}\frac{1}{\sqrt{mkT}}\exp(\frac{E_b}{kT}).$$ (3.33)

We also rewrite the expression in terms of the impinging gaseous flux Φ_{flux},

$$\frac{N}{A_D} = \frac{s}{v_d}\Phi_{flux}\exp(\frac{E_b}{kT}).$$ (3.34)

We derive the spectral density of the fractional frequency noise by considering the dilute gas limit of Yong and Vig's model. This is done by keeping the number of adsorbed molecules, $N = fN_a$, constant, and letting the occupational probability go to zero, and N_a go to infinity. Hence, $\sigma_{OCC}^2 N_a = f(1-f)N_a \rightarrow N$. The spectral density of fractional frequency noise becomes

43

$$S_y(\omega) = \frac{2N/\pi}{1+(\omega\tau_r)^2}\left(\frac{m}{2M_{eff}}\right)^2.$$ (3.35)

The correlation time due to adsorption-desorption cycle is given by the time constant of the rate equation

$$\frac{dN}{dt} = R_a - R_d = R_a - \nu_d \exp(-\frac{E_b}{kT})N.$$ (3.36)

We find that

$$\tau_r = \nu_d \exp(\frac{E_b}{kT}).$$ (3.37)

Since the spectral density of fractional frequency in equation (3.35) exhibits Lorentizian function form, we use equation (2.16) to obtain

$$\sigma_A(\tau_A) = \sqrt{N}\frac{m}{M_{eff}}\sqrt{F(\frac{\tau_r}{\tau_A})}.$$ (3.38)

In the limit, $\tau_r \ll \tau_A$, this expression becomes

$$\sigma_A(\tau_A) = \sqrt{N}\frac{m}{M_{eff}}\sqrt{\frac{\tau_r}{2\tau_A}}.$$ (3.39)

In the other limit, $\tau_A \ll \tau_r$, this expression becomes

$$\sigma_A(\tau_A) = \sqrt{N}\frac{m}{M_{eff}}\sqrt{\frac{\tau_A}{6\tau_r}}.$$ (3.40)

Table 3.3 tabulates the expressions for the two models presented here. Note that equation (3.27) differs from equation (3.38) in the statistics. The occupational variance σ_{OCC}^2 in equation (3.27) and thus adsorption-desorption noise in Yong and Vig's model vanishes upon completion of one monolayer due to the assumption that each site accommodates

only one molecule. In contrast, equation (3.38) exhibits idea gas statistics, manifested in the square root dependence of the number of adsorbed molecules.

Now we discuss the effect of the correlation time on Allan deviation. Because the spectral density of fractional frequency for these two models exhibits Lorentizian functional form, both equation (3.27) and equation (3.38) have the same dependence on the ratio of the correlation time, τ_r, to the averaging time, τ_A, through the analytic function, $F(x)$, defined in equation (2.17). Mathematically, $F(x)$ reaches a maximum at 0.095 for x=1.85 and vanishes when x equals to zero or infinity, and. In other words, the adsorption-desorption noise in both models maximizes when $\tau_r = 0.095\tau_A$ and diminishes for $\tau_r \gg \tau_A$ or $\tau_r \ll \tau_A$ with the asymptotic behaviors dictated by equation (3.25), equation (3.26), equation (3.37), and equation (3.38).

To explicitly illustrate the surface effect of adsorption-desorption noise, we give the expression for the maximum Allan deviation $\sigma_{A\max}$ in Yong and Vig's model by simultaneously maximizing σ_{OCC} and $F(\tau_r / \tau_A)$ in equation (3.27). We find that

$$\sigma_{A\max} = 0.3\frac{\sqrt{N_a}m}{N_a m_D} = 0.3\left(\frac{m}{m_D}\right)\frac{\sqrt{N_a}}{N_V} = 0.3\left(\frac{m}{m_D}\right)\frac{1}{\sqrt{N_V}}\frac{N_a}{N_V} . \tag{3.41}$$

Here m_D is the mass of a single atom adsorbed the device. N_V is the total number of atoms of the device. N_a / N_V is the surface-to-volume ratio.

Finally, we give the expressions for minimum measurable frequency shift and mass sensitivity. For Yong and Vig's model, the integration of the spectra density yields

$$\delta\omega_0 = \frac{1}{2\pi}\frac{m\omega_0\sigma_{occ}}{M_{eff}}\left[N_a \arctan(2\pi\Delta f\tau_r)\right]^{1/2} , \tag{3.42}$$

$$\delta M \approx \frac{1}{2\pi} m \sigma_{occ} \left[N_a \arctan(2\pi \Delta f \tau_r) \right]^{1/2} . \tag{3.43}$$

Similar to equation (3.41), we give the expression for the maximum mass fluctuation δM_{max} by the maximized σ_{OCC} and $\arctan(2\pi \Delta f \tau_r)$ in equation (3.43) from Yong and Vig's model. We find that $\delta M_{max} \approx 1/\sqrt{32\pi} \sqrt{N_a} m$ when $2\pi \Delta f \tau_r \to \infty$ and $f = 0.5$.

Similarly, for ideal gas model, we obtain

$$\delta \omega_0 = \frac{1}{2\pi} \frac{m \omega_0}{M_{eff}} \left[N \arctan(2\pi \Delta f \tau_r) \right]^{1/2} , \tag{3.45}$$

$$\delta M \approx \frac{1}{2\pi} m \left[N \arctan(2\pi \Delta f \tau_r) \right]^{1/2} . \tag{3.46}$$

Table 3.2 summarizes the expressions from Yong and Vig's and ideal gas models. Table 3.3 shows the numerical estimates of $\sigma_{A max}$ and δM_{max} arising from nitrogen for the same representative NEMS devices used in table 3.1. (The number of sites, N_a, is calculated assuming each atom on the device surface serves as one adsorption site. For silicon beam and nanowire, we assume that the device surface is terminated Si(100) with lattice constant=5.43 Å. For a single-walled nanotube (SWNT), we assume that the carbon bond length is 1.4 Å.) First, the magnitude of δM_{max} indicates that the mass fluctuation associate with adsorption-desorption noise of NEMS is at zeptogram level. Second, table 3.4 shows the increase of Allan deviation as a result of increasing the surface-to-volume ratio as the device dimensions are progressively scaled down. In particular, for the 10 GHz single-walled nanotube (SWNT), representing the extreme case that all the atoms are on the surface, the corresponding Allan deviation is almost five orders of magnitude higher than that due to thermomechanical noise (see table 3.1). In other words, the adsorption-desorption noise can severely degrade the noise performance

of the device. This, however, can be circumvented by packaging the device at low pressure or passivating the device surface.

Table 3.2. Summary of Yong and Vig's and ideal gas models

	Yong and Vig	Ideal Gas
Adsorption	Localized	Delocalized
Rates	$r_a = \dfrac{2}{5}\dfrac{p}{\sqrt{mkT}}sA_{Site}$ $r_d = \nu_d \exp(E_b/k_BT)$	$R_a = \dfrac{2}{5}\dfrac{p}{\sqrt{mk_BT}}sA_D$ $R_d = \nu_d \exp(E_b/k_BT)N$
Isotherm	$\dfrac{N}{N_a} = \dfrac{a(T)p}{1+a(T)p}$ $a(T) = \dfrac{2}{5}\dfrac{s}{\sqrt{mkT}\nu_d}\exp(\dfrac{E_b}{kT})A_{site}$	$\dfrac{N}{A_D} = b(T)p$ $b(T) = \dfrac{2}{5}\dfrac{s}{\sqrt{mkT}\nu_d}\exp(\dfrac{E_b}{kT})$
Correlation Time	$\tau_r = 1/(r_a + r_d)$	$\tau_r = 1/\nu_d \exp(E_b/kT)$
Spectral Density	$S_y(\omega) = \dfrac{2N_a\sigma_{OCC}^2\tau_r/\pi}{1+\omega^2\tau_r^2}\left(\dfrac{m}{M_{eff}}\right)^2$	$S_y(\omega) = \dfrac{2N\tau_r/\pi}{1+\omega^2\tau_r^2}\left(\dfrac{m}{M_{eff}}\right)^2$
Allan deviation	$\sigma_A = \sigma_{OCC}\sqrt{N_a}\dfrac{m}{M_{eff}}\sqrt{\dfrac{\tau_r}{2\tau_A}}$ $\sigma_{OCC}^2 = r_a r_d /(r_a+r_d)^2$	$\sigma_A = \sqrt{N}\dfrac{m}{M_{eff}}\sqrt{\dfrac{\tau_r}{2\tau_A}}$

Device	Frequency	N_α/N_V	Na	$\sigma_{\text{Amax}}(\text{gas})$	δM_{max}
Si beam	1 GHz	1.1×10^{-2}	8.9×10^{5}	1.7×10^{-6}	1.6 zg
Si nanowire	7.7 GHz	5.5×10^{-2}	2.7×10^{4}	4.9×10^{-5}	0.28 zg
SWNT	10 GHz	1	5.0×10^{3}	4.9×10^{-3}	0.27 zg

Table 3.3. Maximum Allan deviation and mass fluctuation of representative NEMS devices

3.5 Diffusion Noise

So far we have analyzed the adsorption-desorption noise from adsorbed gasous species on the NEMS device. The surface diffusion provides another channel for exchange of adsorbed species between the device and the surroundings to generate noise. We start the analysis of diffusion noise from calculating the autocorrelation function of fractional frequency fluctuation. Mathematically, the autocorrelation function $G(\tau)$ is calculated as the time average ($<>$) of the product of the frequency fluctuations of the NEMS.

$$G(\tau) =< \delta f(t)\delta f(t+\tau) > / < f(t) >^2 =< \int \delta f(x,t)dx \int \delta f(x',t+\tau)dx' > / < f(t) >^2 . \quad (3.47)$$

Here $f(t)$ is the instantaneous resonant frequency of the device and we define the averaged resonant frequency by $< f(t) >\equiv f_0$. In the actual experiments, $\delta f(x,t)$ remains proportional to local concentration fluctuation $\delta C(x,t)dx$ and is given by

$$\frac{\delta f(x,t)}{f_0} = -\frac{m}{2M_{eff}}\frac{u(x)^2 \delta C(x,t)dx}{\frac{1}{L}\int u(x)^2 dx}, \quad (3.48)$$

where m is the mass of the adsorbed atoms or molecules, M_{eff} is the effective vibratory mass of the device,[3] L is the length of the device, and $u(x)$ is the eigenfunction describing flexural displacement of the beam. Here we only consider the fundamental mode $u(x) = 0.883\cos kx + 0.117\cosh kx$ for a beam extending from $-L/2$ to $L/2$, with $kL = 4.730$ with doubly clamped boundary condition imposed. Note that the end of the beam is never perfectly clamped so doubly clamped boundary condition is only an approximation. The normalization of $u(x)$ factors out in equation (3.48); therefore we are

free to choose $u(0)=1$. We define Green function for diffusion as $\phi(x,x',\tau)=<\delta C(x,t+\tau)\delta C(x',t)>$. As a result, equation (3.48) becomes

$$G(\tau)=L^2(\frac{m}{2M_{eff}})^2=L^2(\frac{m}{2M_{eff}})^2\frac{\int_{-L/2}^{L/2}dx\int_{-L/2}^{L/2}dx'u(x)^2u(x')^2\phi(x,x',t)>}{\left[\int_{-L/2}^{L/2}u(x)^2\,dx\right]^2}.$$ (3.49)

In case of pure diffusion of one species in one dimension, the concentration $\delta C(x,\tau)$ obeys the diffusion equation

$$\frac{\partial\delta C(x,\tau)}{\partial\tau}=D\frac{\partial^2\delta C(x,\tau)}{\partial^2 x}.$$ (3.50)

Following Elson and Magde,[19,20] we find that

$$\phi(x,x',\tau)=\frac{N}{L}\frac{1}{\sqrt{4\pi D\tau}}\exp[-\frac{(x-x')^2}{4D\tau}],$$ (3.51)

where N is the average total number of the adsorbed atoms inside the device. To calculate the autocorrelation function, we can approximate the vibrational mode shape $u(x)$ by a Gaussian mode shape $\exp[-\frac{1}{2}(\frac{ax}{L})^2]$ with a numerical factor $a=4.43$, extending from $-\infty$ to ∞. Figure 3.1 shows the true vibration mode shape of the beam with its Gaussian approximation. Using Gausssian approximation, we can perform the integral analytically and obtain the autocorrelation function of the fractional frequency noise

$$G(\tau)=L^2(\frac{m}{2M_{eff}})^2\int_{-L/2}^{L/2}dx'\int_{-L/2}^{L/2}dx[u(x)^2u(x')^2\phi(x,x',\tau)/\left[\int_{-L/2}^{L/2}u(x'')^2\,dx''\right]^2$$

$$\approx L^2(\frac{m}{2M_{eff}})^2\int_{-\infty}^{\infty}dx\int_{-\infty}^{\infty}dx'[u(x)^2u(x')^2\phi(x,x',\tau)/\left[\int_{-\infty}^{\infty}u(x'')^2\,dx''\right]^2$$ (3.52)

$$=\frac{aN}{\sqrt{2\pi}}(\frac{m}{2M_{eff}})^2\frac{1}{(1+\tau/\tau_D)^{1/2}}.$$

Here the diffusion time is defined by $\tau_D = L^2 /(2a^2 D)$. Note that the time course of $G(\tau)$ is determined by the factor $(1+\tau/\tau_D)^{-1/2}$ even if the concentration correlation function has a typical exponential time dependence. This results from the convolution of the exponential Fourier components of diffusion with the Gaussian profile of the mode shape.[20] Also note that $G(\tau)$ is of the form $(1+\tau/\tau_D)^{-1/2d}$ with $d=1$, the dimensionality of the problem. This is consistent with the factor $(1+\tau/\tau_D)^{-1/2d}$, obtained by Elson and Magde with $d=2$.

We then apply the Wiener-Khintchine theorem to obtain the corresponding spectral density by

$$S_y(\omega) = \frac{1}{\pi}\int_{-\infty}^{\infty} G(\tau)e^{i\omega\tau} = \frac{\sqrt{2}aN}{\pi^{3/2}}(\frac{m}{2M_{eff}})^2 \int_0^{\infty} \frac{\cos\omega\tau}{(1+\tau/\tau_D)^{1/2}} d\tau$$
$$= \frac{aN}{4\pi}(\frac{m}{M_{eff}})^2 \tau_D \xi(\omega\tau_D).$$

(3.53)

Here $\xi(x) \equiv (\cos(x)+\sin(x)-2C(\sqrt{x})\cos(x)-2S(\sqrt{x})\sin(x))/\sqrt{x}$ and $C(x)$ and $S(x)$ are Fresnel integrals defined by[21]

$$C(x) = \sqrt{\frac{2}{\pi}}\int_0^x \cos u^2 du,$$

(3.54)

$$S(x) = \sqrt{\frac{2}{\pi}}\int_0^x \sin u^2 du.$$

(3.55)

In figure 3.2, we plot the function $\xi(x)$ with its asymptotic forms: $\xi(x)=1/\sqrt{x}$ as $x \to 0$ and $\xi(x)=1/x^2\sqrt{2\pi}$ as $x \to \infty$. For $\omega << 1/\tau_D$, the spectral density of fractional frequency noise is given by

$$S_y(\omega) = \frac{aN}{4\pi}(\frac{m}{M_{eff}})^2 \tau_D \frac{1}{\sqrt{\omega\tau_D}}.$$

(3.56)

For $\omega \gg 1/\tau_D$, the spectral density of fractional frequency noise is given by

$$S_y(\omega) = \frac{a}{4\sqrt{2}\pi^{3/2}} N(\frac{m}{M_{eff}})^2 \frac{1}{\omega^2 \tau_D}.$$ (3.57)

We now obtain the expression for Allan deviation using equation (3.53) by the performing the following integration,

$$\sigma_A^2(\tau_A) = \int_0^\infty \frac{8}{(\omega\tau_A)^2} S_y(\omega) \sin^4(\omega\tau_A/2) d\omega = \frac{2aN}{\pi} \left(\frac{m}{M_{eff}}\right)^2 X(\frac{\tau_D}{\tau_A}).$$ (3.58)

Here $X(x)$ is defined as

$$X(x) = x \int_0^\infty \xi(\eta x) \frac{\sin^4(\eta/2)}{\eta^2} d\eta.$$ (3.59)

For $x \to \infty$, the asymptotic form of $X(x)$ is given by

$$X(x) = \frac{\pi^{1/2}}{24\sqrt{2}} \frac{1}{x}.$$ (3.60)

In figure 3.3, we plot the function $X(x)$ in equation (3.60) together with its asymptotic form. For the limit, $\tau_D \gg \tau_A$, we give the expression for Allan deviation as[1]

$$\sigma_A^2(\tau_A) = \int_0^\infty \frac{8}{(\omega\tau_A)^2} S_y(\omega) \sin^4(\omega\tau_A/2) d\omega = \frac{aN}{12\pi} \left(\frac{m}{M_{eff}}\right)^2 \frac{\tau_A}{\tau_D}.$$ (3.61)
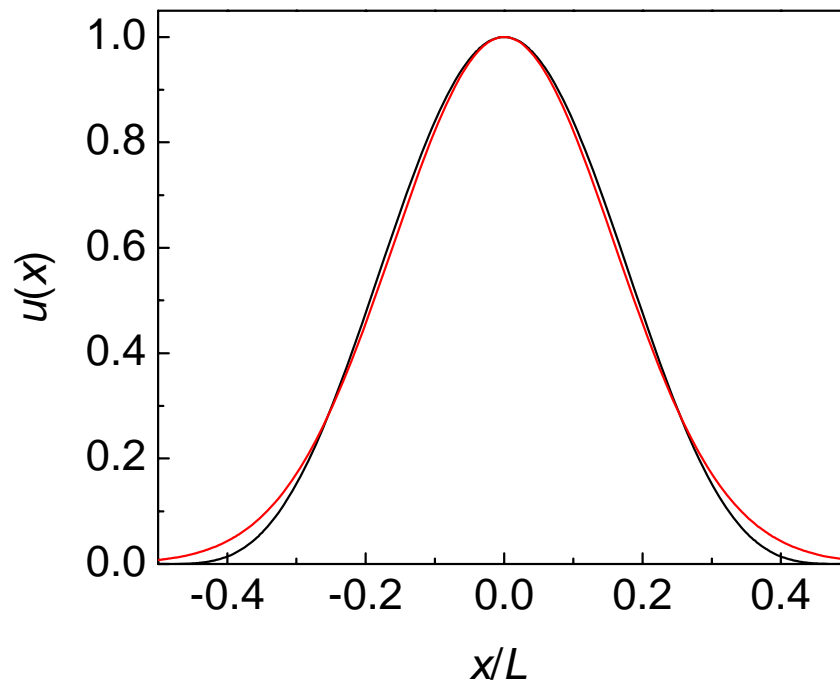
Figure 3.1. Vibrational mode shape of the beam with doubly clamped boundary condition imposed and its Gaussian approximation. The vibrational beam mode shape (black) with doubly clamped boundary condition imposed is displayed with its Gaussian approximation (red).
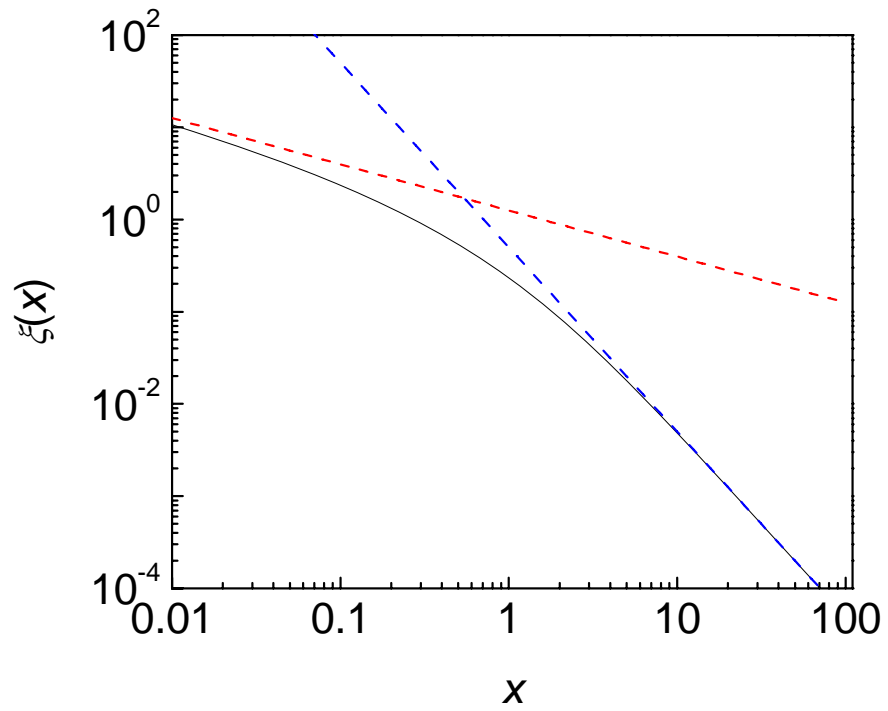
Figure 3.2. Plot of the function $\xi(x)$. The function $\xi(x)$ (black solid) is plotted together with it asymptotic approximations $1/\sqrt{x}$ (red dash) as $x \to 0$ and $1/x^2\sqrt{2\pi}$ (blue dash) as $x \to \infty$.
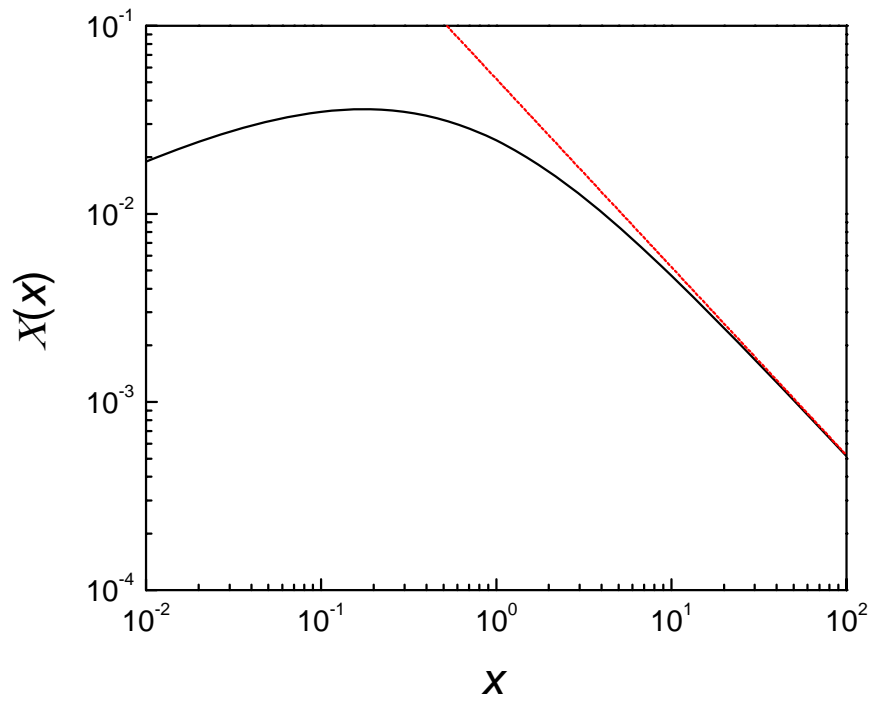
Figure 3.3. Plot of $X(x)$ and its asymptotic form. The function $X(x)$ (black solid) is plotted together with its asymptotic form (red dash) $X(x) = \dfrac{\pi^{1/2}}{24\sqrt{2}} \dfrac{1}{x}$ as $x \to \infty$.

3.6 Temperature Fluctuation Noise

The small dimensions of NEMS resonators in general imply that the heat capacity is very small and therefore the corresponding temperature fluctuations can be rather large. The effect of such fluctuations depends on upon the thermal contact of the NEMS to their environment. Because the resonant frequency depends on the temperature through the resonator material parameters and geometric dimensions, the temperature fluctuations produce frequency fluctuations. Here we present a simple model using the thermal circuit consisting of a heat capacitance, c, connected by a thermal conductance, g, to an infinite thermal reservoir at temperature, T. In the absence of any power load, the heat capacitance, c, will have an average thermal energy, $\langle E_C \rangle = cT$. Changes in temperature relax with thermal time constant, $\tau_T = c/g$. Applying the fluctuation-dissipation theorem to such a circuit, we expect a power noise source, p, connected to the thermal conductance, g, with the spectral density, $S_p(\omega) = 2k_B T^2 g / \pi$, and cause the instantaneous energy, $E_C(t) = \langle E_C \rangle + \delta E(t)$, to fluctuate.[4] The spectral density of the energy fluctuations $\delta E(t)$ can be derived as

$$S_E(\omega) = \frac{2}{\pi} \frac{k_B T^2 c^2 / g}{1 + \omega^2 \tau_T^2}.$$
(3.62)

We can interpret the energy fluctuations as temperature fluctuations $\delta T_C(t)$, if we define the temperature as $T_C = E_C / c$. The corresponding spectral density of the temperature fluctuations is given by

$$S_T(\omega) = \frac{2}{\pi} \frac{k_B T^2 / g}{1 + \omega^2 \tau_T^2}.$$
(3.63)

57

Equation (3.63) applies to any system that can be modeled as a heat capacitance with a thermal conductance. For a doubly clamped beam, however, there is no clear separation of the structure into a distinct heat capacitance and a thermal conductance. Cleland and Roukes have developed a distributed model of thermal transport along a doubly clamped beam of constant cross section, and derived the spectral density of frequency fluctuations arising from temperature fluctuations of a NEMS resonator.[1] Their analysis leads to

$$S_T(\omega) = \frac{4}{\pi} \frac{k_B T^2 / g}{1 + \omega^2 \tau_T^2},$$

(3.64)

$$S_y(\omega) = \left(-\frac{22.4}{\omega_0^2 L^2} \alpha_T + \frac{2}{c_s} \frac{\partial c_s}{\partial T} \right)^2 \frac{1}{\pi} \frac{k_B T^2 / g}{1 + \omega^2 \tau_T^2}.$$

(3.65)

Here $c_s = \sqrt{E / \rho}$ is the temperature dependent speed of sound, $\alpha_T = (1/L)\partial L / \partial T$ is the linear thermal expansion coefficient, and g and τ_T are the thermal conductance and thermal time constant for the slice, respectively. In the limits $\tau_A \gg \tau_T$, the Allan deviation is given by

$$\sigma_A(\tau_A) = \sqrt{\frac{2 k_B T^2}{g \tau_A} \frac{1}{\tau_T} \left(-\frac{22.4}{\omega_0^2 L^2} \alpha_T + \frac{2}{c_s} \frac{\partial c_s}{\partial T} \right)^2}.$$

(3.66)

To give the expression for $\delta\omega_0$ and δM, we integrate equation (3.65) over the measurement bandwidth and obtain

$$\delta\omega_0 = \left[\frac{1}{2\pi^2} \left(-\frac{22.4 c_s^2}{\omega_0^2 l^2} \alpha_T + \frac{2}{c_s} \frac{\partial c_s}{\partial T} \right)^2 \frac{\omega_0^2 k_B T^2}{g} \frac{\arctan(2\pi \Delta f \tau_T)}{\tau_T} \right]^{1/2},$$

(3.67)

$$\delta M = \frac{2}{\pi^{1/2}} 2M_{eff} \left(-\frac{22.4c_s^2}{\omega_0^2 l^2}\alpha_T + \frac{2}{c_s}\frac{\partial c_s}{\partial T} \right) \left[\frac{k_B T^2 \arctan(2\pi\Delta f \tau_T)}{g\tau_T} \right]^{1/2}. \qquad (3.68)$$

The values of the material dependent constants for silicon have been calculated as[1]

$$\left(-\frac{22.4}{\omega_0^2 L^2}\alpha_T + \frac{2}{c_s}\frac{\partial c_s}{\partial T} \right)^2 = 1.26\times 10^{-4}\ 1/K. \qquad (3.69)$$

$g = 7.4\times 10^{-6}$ W/K and $\tau_T = 30$ ps. Using these values, a numerical estimate of equation (3.66) for 1 GHz silicon beam in table 3.1 is given by $\sigma_A(\tau_A) = 9.3\mathrm{x}10^{-11}/\sqrt{\tau_A}$.[1] For $\tau_A = 1$ sec, the Allan deviation is $9.3\mathrm{x}10^{-11}$, of the same order of magnitude as that due to the thermomechanical noise at room temperature listed in table 3.1. Similarly, for the same device at room temperature with measurement bandwidth $\Delta f = 1$ Hz, we obtain $\delta M = 0.245$ Da. Despite of the role of thermal fluctuations in generating phase noise that limits the mass sensitivity, single Dalton sensing is readily achievable. The effect can be even more significant as we further scale down the dimensions or increase the device temperature. This can be circumvented by lowering the temperature or optimizing the thermal contact of the NEMS to its environment.

3.7 Nonfundamental Noise

We develop a simple formalism to consider nonfundamental noise process from transducer amplifier implementations of NEMS.[5] First, the spectral density of the frequency noise $S_\omega(\omega)$ is transformed into the voltage domain by the displacement

transducer, the total effective voltage noise spectral density at the transducer's output predominantly originates from the transducer and readout amplifier.[5] It is the total voltage noise referred back to the frequency domain that determines the effective frequency fluctuation spectral density for the system $S_\omega(\omega) = S_V /(\partial V / \partial \omega)^2$. V is the transducer output voltage. If we define the transducer responsivity by the derivative of transducer output voltage with respect to displacement, i.e., $R_T = (\partial V / \partial x)$, a simple estimate is given by $(\partial V / \partial \omega) \approx Q R_T |x_C| / \omega_0$. Assuming the voltage fluctuation S_V results from Nyquist-Johnson noise from the transducer amplifier and thus has a white spectrum, using equation (2.15) we obtain the expression for the Allan deviation

$$\sigma_A(\tau_A) = \frac{1}{Q} \frac{(\pi S_V / \tau_A)^{1/2}}{R_T |x_C|}. \tag{3.70}$$

We can rewrite this equation in a simple form in terms of the dynamic range, $DR = 20 \log[R_T^2 |x_C|^2 /(\pi S_V / \tau_A)^{1/2}]$, or equivalently the signal-to-noise ratio (SNR) referred to transducer output of the NEMS.

$$\sigma_A(\tau_A) = \frac{1}{Q} 10^{-DR/20}. \tag{3.71}$$

Finally, we give the expression for the minimum detectable frequency shift $\delta\omega$ and mass sensitivity δM. Upon the integration of spectral density using equation (2.21), the minimum detectable frequency shift for the measurement bandwidth Δf, is simply

$$\delta\omega = \frac{\omega_0}{Q} \frac{(S_V \Delta f)^{1/2}}{R_T |x_C|} = \frac{\omega_0}{Q} 10^{-DR/20}. \tag{3.72}$$

The mass sensitivity follows as

$$\delta M \sim 2(M_{eff} / Q) 10^{-DR/20}. \tag{3.73}$$

Equation (3.73) indicates the essential considerations for optimizing NEMS based mass sensors limited by the Nyquist-Johnson noise. First, this emphasizes the importance of devices possessing low mass, i.e., small volume, while keeping high Q. Second, the dynamic range for the measurement should be maximized. This latter consideration certainly involves careful engineering to minimize the noise from transducer amplifier implementations and controlling the nonlinearlity of the resonator through the mechanical design.

3.8 Conclusion

We present the theory of phase noise mechanisms affecting NEMS. We examine both *fundamental* and *nonfundamental* noises and their imposed limits on device performance. Table 3.4 tabulates the expressions for fundamental noise processes considered in this work. We find that the anticipated noise is predominantly from thermomechanical noise, temperature fluctuation noise, adsorption-desorption noise, and diffusion noise. First, a large dynamic range is always desirable for obtaining frequency stability in the case of thermomechanical noise. Clearly, as the device sizes are scaled downward while maintaining high resonance frequencies, M_{eff} and κ_{eff} must shrink in direct proportion. Devices with small stiffness (high compliance) are more susceptible to thermal fluctuations and consequently, the dynamic range becomes reduced. Second, next generation NEMS appear to be more susceptible to temperature fluctuations—more intensively at elevated temperatures. This fact can be circumvented by lowering the device temperatures and by designing NEMS with better thermalization properties. Third, for adsorption-desorption noise, both Yong and Vig's and ideal gas model suggest that

this noise becomes significant when appreciable molecules adsorb on the NEMS surface and the correlation time of adsorption-desorption cycle roughly matches the averaging time. One could easily prevent this, for instance, by reducing the packaging pressure or passivating the device to change the binding energy between the molecule and the surface.

To evaluate the impact of each noise process on the mass sensing application, we give expressions for the minimum measurable frequency shift and mass sensitivity. Our analysis culminates in the expression equation (3.10), i.e.,

$$\delta M \approx \frac{1}{\Re} \left(\Delta f \frac{\omega_0}{Q} \right)^{1/2} 10^{(-DR/20)} . \tag{3.74}$$

Equation (3.74) distills and makes transparent the essential considerations for optimizing inertial mass sensors at any size scale. There are three principal considerations. First, the mass responsivity, $\Re$, should be maximized. As seen from equation (3.3), this emphasizes the importance of devices possessing low mass, i.e., small volume, which operate with high resonance frequencies. Second, the measurement bandwidth should employ the full range that is available. Third, the dynamic range for the measurement should be maximized. At the outset, this latter consideration certainly involves careful engineering to minimize nonfundamental noise processes from the transducer amplifier implementation, as expressed in equation (3.72) and equation (3.73). But this is ultimately feasible only when fundamental limits are reached. In such a regime it is the fundamental noise processes that become predominant.

In table 3.1, we have translated the analytical results from equation (3.10) into concrete numerical estimates for representative and realizable device configurations. The values of δM span only the regime from a few tenths to a few tens of Daltons. This is the

mass range for a small *individual* molecule; hence it is clear that nanomechanical mass sensors offer unprecedented sensitivity to *weigh* individual neutral molecules routinely—blurring the distinction between conventional inertial mass sensing and mass spectrometry.[11]

Table 3.4 Summary of expressions for spectral density and Allan deviation for fundamental noise processes considered in this work

Noise	Correlation Time	Expression
Thermomechanical	None	$S_\phi(\omega) = \dfrac{k_B T}{8\pi P_c Q^2}\left(\dfrac{\omega_0}{\omega}\right)^2$ $\sigma_A(\tau_A) = \sqrt{\dfrac{k_B T}{8 P_C Q^2 \tau_A}}$
Momentum Exchange	None	$S_\phi(\omega) = \dfrac{k_B T}{8\pi P_c Q_{gas}^{\;2}}\left(\dfrac{\omega_0}{\omega}\right)^2$ $\sigma_A(\tau_A) = \sqrt{\dfrac{k_B T}{8 P_C Q_{gas}^2 \tau_A}}$
Adsorption-Desorption Yong and Vig's Model	$\tau_r = 1/(r_a + r_d)$	$S_y(\omega) = \dfrac{2\sigma_{OCC}^2 N_a \tau_r / \pi}{1 + \omega^2 \tau_r}\left(\dfrac{m}{2M_{eff}}\right)^2$ $\sigma_A(\tau_A) = \sqrt{N_a}\,\dfrac{\sigma_{OCC} m}{M_{eff}}\sqrt{F(\dfrac{\tau_r}{\tau_A})}$
Ideal Gas Model	$\tau_r = 1/\nu_d \exp(E_b/k_B T)$	$S_y(\omega) = \dfrac{2N\tau_r / \pi}{1 + \omega^2 \tau_r}\left(\dfrac{m}{2M_{eff}}\right)^2$ $\sigma_A(\tau_A) = \sqrt{N}\,\dfrac{m}{M_{eff}}\sqrt{F(\dfrac{\tau_r}{\tau_A})}$
Diffusion	$\tau_D = L^2 / 2a^2 D$	$\sigma_A(\tau_A) = \dfrac{2aN}{\pi}\left(\dfrac{m}{M_{eff}}\right)^2 X(\dfrac{\tau_D}{\tau_A})$
Temperature Fluctuation	$\tau_T = c/g$	$S_y(\omega) = \left[\dfrac{1}{\omega_0}\left(\dfrac{\partial \omega_0}{\partial T}\right)\right]_T^2 \dfrac{4}{\pi}\dfrac{k_B T/g}{1 + \omega^2 \tau_T^2}$ $\sigma_A(\tau_A) = \sqrt{\dfrac{4 k_B T}{g\tau_A}}\,\dfrac{1}{\tau_T}\dfrac{1}{\omega_0}\left(\dfrac{\partial \omega_0}{\partial T}\right)$

References

1.   A. N. Cleland and M. L. Roukes Noise processes in nanomechanical resonators. *J. Appl. Phys.* **92**, 2758 (2002).

2.   J. Vig and Y. Kim Noise in MEMS resonators. *IEEE Trans. on Ultrasonics Ferroelectics and Frequency Control.* **46**, 1558 (1999).

3.   K. L. Ekinci, Y. T. Yang, M. L. Roukes Ultimate limits to inertial mass sensing based upon nanoelectromechanical systems. *J. Appl. Phys.* **95**, 2682 (2004).

4.   L. D. Landau and E. M. Lifshitz *Statistical Physics* (England, Oxford, 1980).

5.   K. L. Ekinci, X. M. H. Huang, and M. L. Roukes Ultrasensitive nanoelectromechanical mass detection. *Appl. Phys. Lett.* **84**, 4469 (2004).

6.   For the fundamental mode response of a doubly clamped beam with rectangular cross section, the effective mass, dynamic stiffness are given as $M_{eff} = 0.735ltw\rho$, $\kappa_{eff} = 32Et^3w/L^3$. Here, *L*, *w*, and *t* are the length, width and thickness of the beam. *E* is Young's modulus and ρ is the mass density of the beam. We have assumed the material is isotropic; for single-crystal device anisotropy in the elastic constants will result in a resonance frequency that depends upon specific crystallographic orientation.

7.   G. Z. Sauerbrey Verwendung von Schwingquarzen zur Wagang dunner Schichten und zur Mikrowagung *Z. Phys.* **155**, 206-222 (1959).

8.   H. A. C. Tilmans and M. Elwenspoek, and H. J. Flutiman Micro resonator force gauge. *Sens. Actuators* **A 30**, 35 (1992).

9.   For a doubly clamped tube of diameter d, we can calculate the maximum carrier power using $|x_C| = d/\sqrt{2}/\sqrt{0.5Q(1-v^2)}$. See A. Husain et al. Nanowire-based very high frequency electromechanical resonator. Appl. Phys. Lett. **83**, 1240 (2003).

10.   W. Hansel, P. Hommelhoff, T. W. Hansh, and J. Reichel. Bose-Einstein condensation on microelectronic chips. *Nature* **413**, 498-500 (2001).

11.   R. Aebersold and M. Mann Mass spectrometry-based proteomics. *Nature* **422**, 198-207 (2003).

12.   W. Gerlach *Naturwiss.* **15**, 15 (1927).

13.   G. E. Uhlenbeck and S. A. Goudsmit A problem in brownian motion. *Phys. Rev.* **34**, 145 (1929).

14. Y. K. Yong and J. R. Vig Resonator surface contamination: a cause of frequency fluctuations. *IEEE Trans. on Ultrasonics Ferroelectics and Frequency Control.* **36**, 452 (1989).

15. H. Clark *The Theory of Adsorption and Catalysis* (London, Academic Press, 1970).

16. S. Ross and H. Clark On physical adsorption VI two dimensional critical phenomena of xenon, methane, ethane adsorbed separately on sodium chloride. *J. Am. Chem. Soci.***76**, 4291 (1954).

17. H. J. Kreuzer and Z. W. Gortel *Physisorption Kinetics* (Heidelberg, Springer-Verlag, 1986).

18. S. M. Ross *Stochastic Process* (New York, John Wiley & Sons, 1996).

19. E. L. Elson and D. Magde Fluoresence correlation spectroscopy I concept basis and theory. *Biopolymer* **13**, 1-27 (1974).

20. D. Magde, E. L. Elson, and W. W. Webb Thermodynamic fluctuations in a reacting system- Measurement by fluorescence correlation spectroscopy. *Phys. Rev. Lett.* **29**, 705-708 (1972).

21. I. S. Gradshteyn and I. M. Ryzhik Alan Jefferey, Editor *Table of Integrals, Series, and Products* 5th edition (New York, Academic Press, 1980).